Surface Modification of Armos Fibers with Oxygen Plasma Treatment for Improving Interfacial Adhesion with Poly(phthalazinone ether sulfone ketone) Resin

Jing Wang,[1] Ping Chen,[1,2] Wei Liu,[3] Hong Li,[1] Caixia Jia,[1] Chun Lu,[2] Baichen Wang[2]

[1]*State Key Laboratory of Material Surface Modification by Laser, Ion and Electronic Beams, School of Chemical Engineering, Dalian University of Technology, Dalian 116012, China*
[2]*Center for Composite Materials, Shenyang Institute of Aeronautical Engineering, Shenyang 110034, China*
[3]*Dalian Education University, Dalian 116021, China*

Received 24 August 2009; accepted 23 November 2010
DOI 10.1002/app.33847
Published online 29 March 2011 in Wiley Online Library (wileyonlinelibrary.com).

ABSTRACT: We introduce in this article oxygen plasma treatment as a convenient and effective method for the surface modification of Armos fibers. The effects of oxygen-plasma-treatment power on both the Armos fiber surface properties and Armos-fiber-reinforced poly(phthalazinone ether sulfone ketone) composite interfacial adhesion were investigated. The Armos fiber surface chemical composition, surface morphology and roughness, and surface wettability as a function of oxygen-plasma-treatment power were measured by X-ray photoelectron spectroscopy, scanning electronic microscopy, atomic force microscopy, and dynamic contact angle analysis. The results show that oxygen plasma treatment introduced a lot of reactive functional groups onto the fiber surface, changed the surface morphology, increased the surface roughness, and enhanced the surface wettability. Additionally, the effect of the oxygen-plasma-treatment power on the composite interfacial adhesion was measured by interlaminar shear strength with a short-beam bending test. Oxygen plasma treatment was an effective method for improving the composite interfacial properties by both chemical bonding and physical effects. © 2011 Wiley Periodicals, Inc. J Appl Polym Sci 121: 2804–2811, 2011

Key words: adhesion; composites; fibers; interfaces; surface

INTRODUCTION

Advanced polymer–matrix composites made from aramid fibers have been widely used in many applications, such as aircraft, automobiles, sporting goods, and medical devices, because the fibers combine a high specific modulus and strength.[1] To exert the excellent mechanical properties of Aramid fibers in composite systems, the optimization of the interfacial adhesion properties between the fiber and the matrix seems to be more necessary. It is well known that the interfacial region plays a major role in the overall mechanical performance of composite materials for transferring stress from the matrix to the fiber under load-bearing conditions. Recently, a few researchers have focused on the analysis of the composite interfacial properties.[2,3]

Poly(phthalazinone ether sulfone ketone) (PPESK) is one kind of novel thermoplastic resin with excellent mechanical properties, high damage tolerance, and remarkable thermal and chemical resistance. Compared with traditional thermoplastic resins, it is provided with the higher heat-resistant grade and better solubility; it can be dissolved in some usual solvents. Thus, fiber-reinforced PPESK composites can be prepared through a solution impregnation technique.[2]

However, the Aramid fiber has poor adhesion with the matrix in the composite system because of its inert chemical structure and smooth surface; this limits the exertion of the composite properties. At this point, several methods have been developed to modify the fiber surface, such as chemical treatment (including coupling agent and chemical grafting methods), surface coating methods, and plasma treatment.[4–10]

Low-temperature plasma treatment has been shown to be an effective method for modifying organic fiber surfaces.[11,12] This method offers several advantages, including the selection modification of only the outer atomic layers of the substrate, the

Correspondence to: P. Chen (chenping_898@126.com).
Contract grant sponsor: National Natural Science Foundation of China; contract grant number: 50743012.
Contract grant sponsor: National Defense 11th 5-Year Program of the Foundational Research Program; contract grant number: A3520060215.
Contract grant sponsor: Innovative Research Team Program in University of Liaoning Education Department; contract grant number: LT2010083.

selection of the desired functional groups, the minimization of thermal degradation, and a rapid treatment time.[13] In recent years, plasma treatments have been more popular than other methods of surface treatment because increasing concern about environmental pollution problems has limited chemical surface treatments.[14]

The objective of this study was to investigate the effects of oxygen-plasma-treatment power on both the Armos fiber surface and Armos-fiber-reinforced PPESK composite interfacial adhesion. The surface chemical composition, surface morphology and roughness, and surface wettability before and after oxygen plasma treatment under different powers were measured by X-ray photoelectron spectroscopy (XPS), scanning electronic microscopy (SEM), atomic force microscopy (AFM), and dynamic contact angle analysis (DCAA), respectively. The influence of oxygen plasma treatment on the composite interfacial adhesion was measured by interlaminar shear strength (ILSS) with a short-beam bending test.

EXPERIMENTAL

Materials

Armos fibers, one kind of high-performance aramid fibers supplied by Tverchimovolokno, J.-S., Russia, were used as the reinforcement in our experiment. They were cleaned successively with acetone and distilled water and then dried in a vacuum oven. The matrix was PPESK supplied by Dalian Polymer New Material Co., Ltd. (Dalian, China). The characteristic viscosity was 0.53, the glass-transition temperature was 284°C, and the molecular structure was reported previously.[2]

Plasma treatment

The plasma was excited by an inductive-coupling, radio-frequency generator (13.56 MHz). The system contained a mass flow controller for an oxygen gas inlet, a pressure gauge, a vacuum pump, and a radio source. Oxygen was fed into the vacuum chamber at a flow rate of about 30–40 cm^3/min. The operation pressure was set at 30 Pa. Fibers were rolled on a glass frame and fixed in a quartz obturator 30 cm in height and 26 cm in inner diameter. After oxygen plasma treatment of the fibers for 10 min under different power levels from 120 to 240 W, the fibers were immediately transferred to a dry box to minimize potential contamination.

Composite specimen preparation

Armos-fiber-reinforced PPESK composites were prepared through a solution impregnating technique according to Chen et al.[15] PPESK resin was dissolved in *N,N*-dimethylacetamide (DMAc) solvent (15 wt %), and then, both the untreated and plasma-treated fibers were soaked with the PPESK/DMAc solution. Monolayer impregnating samples were used to vaporize the DMAc solvent (120°C/1 h, 175°C/3 h, oven) and then made by a compression-molding technique. The volume fraction of Armos fibers in the composite was controlled at about 55%.

Morphology observation by SEM and AFM

The single-fiber surface morphologies were observed by SEM (QUANTA 200, FEI, Netherlands). The chamber pressure was evacuated to a pressure lower than 60 Pa through a molecule pump. The magnification of the image for single fibers was set at 5000×. In addition, the fiber surface morphologies on a microscopic scale (4 × 4 μm^2) were observed by AFM (Picoplus II, America) in tapping (noncontact) mode, and the surface roughnesses, including the root mean square roughness (R_q) and arithmetic mean roughness (R_a), were calculated from eqs. (1) and (2) by the instrument software:

$$R_q = \sqrt{\frac{1}{N^2}\sum_{i=1}^{N}\sum_{j=1}^{N}(z_{ij} - z_{av})^2} \quad (1)$$

$$R_a = \frac{1}{N}\sum_{i=1}^{N}\sum_{j=1}^{N}\left|z_{ij} - z_{cp}\right| \quad (2)$$

where N is the number of data points in the image, i and j are pixel locations on the AFM image, z_{ij} is the height value at i and j locations, z_{av} is the average height value within the given area, and z_{cp} is the height value from the center plane.[16]

Chemical composition analysis by XPS

The fiber surface chemical composition of the Armos fibers were determined by XPS (ESCALAB 250, Thermo, America), with the use of a monochromatic Al Kα ($h\nu$ = 1486.6 eV) X-ray radiation source (voltage = 15 kV, wattage = 250 W) from a dual Al–Mg anode. The vacuum chamber was pumped to lower than 3.0 × 10^{-9} Torr. Spectra were acquired at a takeoff angle of 90° relative to the sample surface. An electron kinetic energy analyzer plotted the intensity of the emitted photoelectrons according to their binding energies. The analyzer was operated in constant-energy mode with a pass energy of 50 eV for elemental quantification purposes. The surface chemical composition was calculated from the areas of relevant spectral peaks. The sampling depth was less than 5 nm.

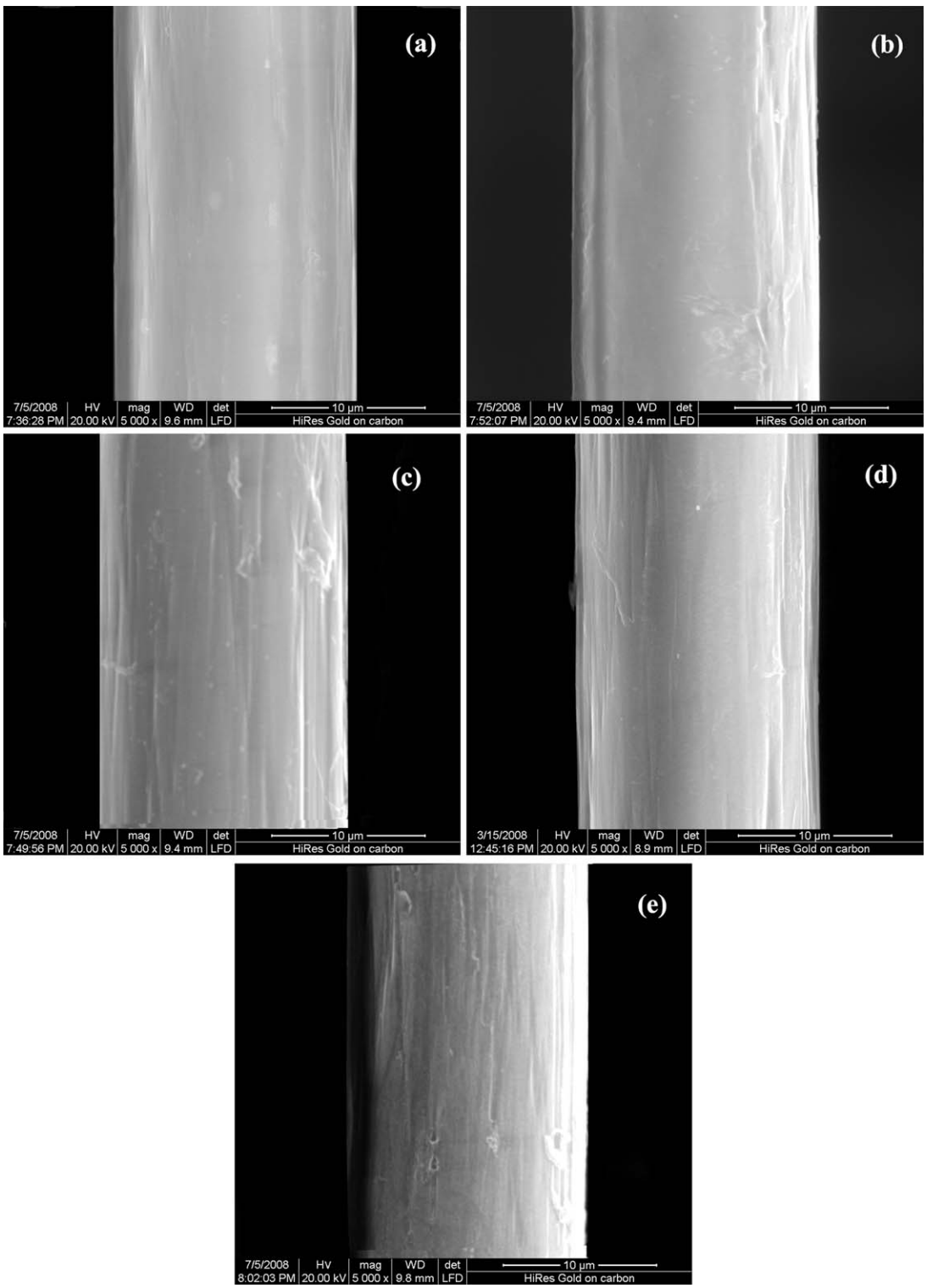

Figure 1 SEM photographs of the Armos fibers: (a) untreated, (b) plasma-treated at 120 W, (c) plasma-treated at 160 W, (d) plasma-treated at 200 W, and (e) plasma-treated at 240 W.

Wettability measured by DCAA

The dynamic contact angle was measured by a Cahn DCA-322 (Thermo, America) analysis system according to the Wilhelmy technique.[17] The fiber sample was cut to about 1 cm in length, fixed indirectly to a wire suspended from a microbalance, and then immersed in the testing liquid medium by an increase in the elevating stage at a constant speed of 1 mm/min. The contact angles were calculated with a computer system with eq. (3). The surface free

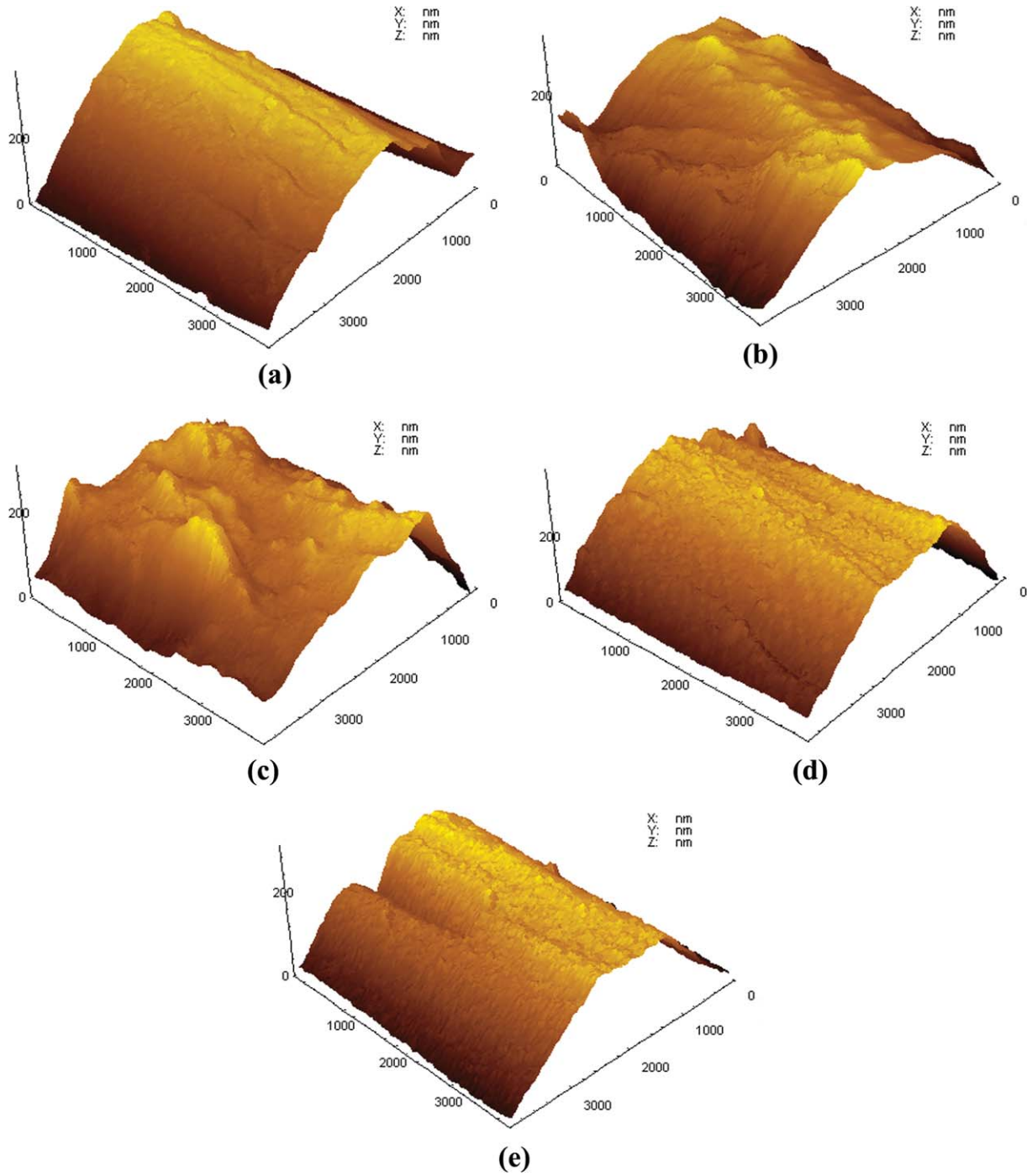

Figure 2 AFM photographs of the Armos fibers: (a) untreated, (b) plasma-treated at 120 W, (c) plasma-treated at 160 W, (d) plasma-treated at 200 W, and (e) plasma-treated at 240 W. [Color figure can be viewed in the online issue, which is available at wileyonlinelibrary.com.]

energy was calculated from the Owens–Wendt equations [eqs. (4) and (5)]:

$$F = \gamma p \cos\theta. \tag{3}$$

$$\gamma_l(1 + \cos\theta) = 2\sqrt{\gamma_s^p \gamma_l^p} + 2\sqrt{\gamma_s^d \gamma_l^d} \tag{4}$$

$$\gamma_{\text{Total}} = \gamma_s^p + \gamma_s^d \tag{5}$$

where F is the wetting force measured by the microbalance, γ is surface free energy, p is the wetted perimeter, θ is the contact angle between the fiber and the liquid, γ_l is the surface tension of the testing liquid, γ_{Total} is the surface free energy of the fiber, and γ_s^p is the polar component and γ_s^d is the dispersive

component of the surface free energy of the fiber.

ILSS measurement

ILSS was measured on a Shimadzu, Japan universal testing machine with a three-point short-beam bending test method according to GB3357-82. The specimen dimensions were $25 \times 6 \times 2$ mm^3, with a span-to-thickness ratio of 5. The specimens were tested at a constant crosshead movement rate of 2 mm/min. ILSS was calculated according to the following expression:

$$\Gamma = \frac{3P_b}{4bh} \quad (6)$$

where Γ is the interlaminar shear strength (MPa), P_b is the maximum compression load at fracture (N), b is the width of the specimen (mm), and h is the thickness of the specimen (mm). Each ILSS value reported was the average of five tested specimens.

RESULTS AND DISCUSSION

Influence of the oxygen-plasma-treatment power on the Armos fiber surface morphology and surface roughness

Figure 1 shows the single-fiber surface morphologies observed by SEM. Compared with the untreated fiber sample in Figure 1(a), the surfaces were roughened after oxygen plasma treatment, as shown in Figure 1(b–e). Furthermore, AFM was used to detect the surface changes on a microscopic scale. The three-dimensional morphological images of the untreated and oxygen-plasma-treated samples under different powers are shown in Figure 2. The results seemed to consistent with the SEM photographs. The fiber surface was clean and smooth for the untreated sample shown in Figure 2(a) and left some streaks caused by the intrinsic structure of the Armos fiber.[18] After plasma treatment at 120 W, some small protrusions were evident, as shown in Figure 2(b); with increasing plasma-treatment power, more and more granules emerged and were well-distributed on the surface, as shown in Figure 2(c,d).

TABLE I
Surface Roughnesses (R_q and R_a) of the Armos Fibers Under Different Plasma-Treatment Powers

Sample	R_q (nm)	R_a (nm)
Untreated	197	180
Plasma-treated at 120 W	229	218
Plasma-treated at 160 W	226	216
Plasma-treated at 200 W	279	261
Plasma-treated at 240 W	195	177

The results indicate that oxygen plasma treatment roughened the fiber surface and led to increases in the contact area with the matrix and the friction between the fiber and the matrix to improve the composite interfacial adhesion. However, as the plasma-treatment power reached 240 W, some big grooves were observed on the surface, as shown in Figure 2(e). This may have been the result of etching effects by the oxygen plasma treatment with prolonged power.

The surface roughnesses, including R_q and R_a, were changed after oxygen plasma treatment, and the results are shown in Table I. R_q increased from 197 nm for the untreated sample to 279 nm for the plasma-treated sample with a power of 200 W. However, with the plasma-treatment power increasing to 240 W, the surface roughness began to decrease; this may have been due to surface ablation under the high plasma-treatment power because the higher plasma-treatment power brought more reactive particles with higher energies and thermal effects on the fiber surface.[19] From the results of SEM and AFM, we found that the oxygen plasma treatment changed the fiber surface morphology and enhanced the surface roughness under the proper power.

Influence of the oxygen-plasma-treatment power on the Armos fiber surface chemical composition

XPS was used to analyze the chemical composition of the Armos fiber surface. Because the sampling depth was less than 5 nm, the surface composition could be very different from the bulk composition. Through calculation of the peak areas of carbon, oxygen, and nitrogen, we obtained the relative

TABLE II
Surface Chemical Compositions of the Armos Fibers Under Different Plasma-Treatment Powers

	Chemical composition (at %)			Atomic ratio	
Sample	C1s	O1s	N1s	O1s/C1s	N1s/C1s
Untreated	81.9	11.1	7.0	0.14	0.09
Plasma-treated at 120 W	69.1	23.3	7.6	0.34	0.11
Plasma-treated at 160 W	71.6	17.4	11.0	0.24	0.15
Plasma-treated at 200 W	73.7	15.2	11.1	0.21	0.15
Plasma-treated at 240 W	71.3	16.3	12.4	0.23	0.17

TABLE III
Contents of the Functional Groups of the Armos Fibers Under Different Plasma-Treatment Powers

Sample	Contents of the functional groups (%)				
	—C—C— (284.5 eV)	—C—N— (285.5 eV)	—C—O— (286.5 eV)	—C=O (287.7 eV)	—COO— (289.2 eV)
Untreated	71.9	12.3	6.7	6.0	3.1
Plasma-treated at 120 W	71.9	11.5	5.0	5.8	5.8
Plasma-treated at 160 W	62.5	16.2	6.9	8.8	5.6
Plasma-treated at 200 W	61.9	13.4	6.6	10.9	7.2
Plasma-treated at 240 W	65.4	8.5	11.1	8.5	6.5

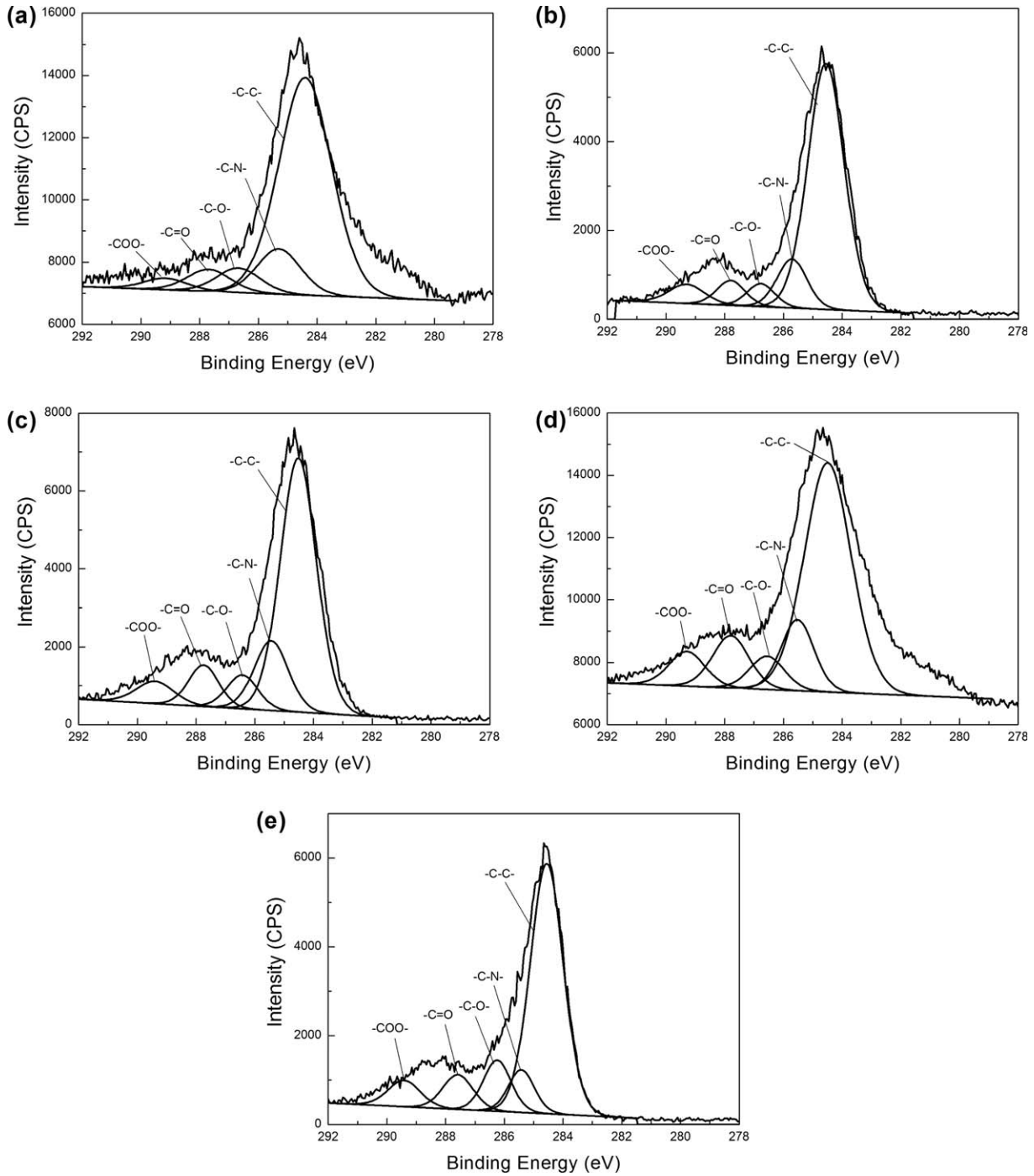

Figure 3 C1s spectra of the Armos fibers: (a) untreated, (b) plasma-treated at 120 W, (c) plasma-treated at 160 W, (d) plasma-treated at 200 W, and (e) plasma-treated at 240 W.

TABLE IV
Contact Angles with Water and Diiodomethane and the Surface Free Energy Values of the Armos Fibers Under Different Plasma-Treatment Powers

Sample	θ (°)[a]		Surface free energy (mJ/m^2)		
	Water	Diiodomethane	γS^p	γS^d	γ total
Untreated	73.7 (2.1)	40.3 (2.3)	6.8	39.4	46.2
Plasma-treated at 120 W	39.6 (2.3)	46.8 (3.7)	27.0	36.0	63.0
Plasma-treated at 160 W	36.8 (1.2)	48.9 (2.8)	29.2	34.9	64.1
Plasma-treated at 200 W	20.9 (0.8)	44.4 (2.3)	35.3	37.3	72.6
Plasma-treated at 240 W	39.4 (5.5)	44.6 (0.7)	26.5	37.2	63.7

[a] Standard deviations are shown in parentheses.

chemical compositions; these are listed in Table II. The surface carbon and oxygen concentrations were 81.9 and 11.1%, and the O/C ratio was 0.14 for the untreated sample. With a plasma-treatment power of 120 W, the surface carbon concentration decreased sharply to 69.1%, the surface oxygen concentration increased obviously to 23.3%, and the O/C ratio increased to 0.34. An explanation is that the oxygen plasma treatment introduced oxygen-containing functional groups onto the fiber surface at lower plasma-treatment powers. Nitrogen seemed to experience a small change before and after plasma treatment under different powers.

Figure 3 shows the C1s spectra of the Armos fibers before and after oxygen plasma treatment under different powers. According to the calculation of each peak area, we obtained the relative content of functional groups, as shown in Table III. Obvious changes in —C=O and —COO— concentrations were detected after oxygen plasma-treatment at more than 160 W; this improved the surface chemical reactivity and then enhanced the chemical bonding between the fiber and the matrix in the composite system.[20]

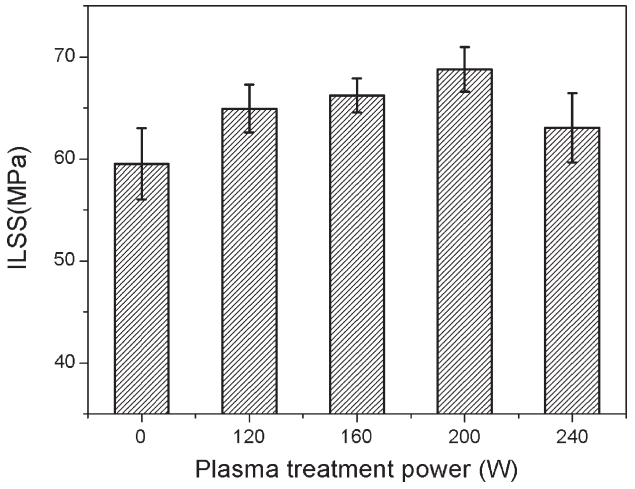

Figure 4 ILSS of the Armos fiber/PPESK composite as a function of the plasma-treatment power.

However, with the plasma-treatment power increasing to 240 W, these two functional group concentrations decreased. We suggest that there existed an optimum plasma-treatment power.

Influence of the oxygen-plasma-treatment power on the Armos fiber surface wettability

The effect of the oxygen-plasma-treatment power on the fiber surface wettability was revealed by dynamic contact angle measurement. From the data in Table IV, we observed that the oxygen plasma treatment was quite effective in modifying the fiber surface. The contact angle with water decreased sharply after plasma treatment, whereas the diiodomethane contact angle increased. Moreover, the polar component for the plasma-treated sample was higher than that of the untreated one. This phenomenon may have been due to many active functional groups introduced onto the fiber surface by plasma, as shown in XPS analysis. The high polar component of the total surface free energy was expected to contribute to good wettability and adhesion between the fiber and the matrix.[14]

Influence of the oxygen-plasma-treatment power on the Armos-fiber-reinforced PPESK composite interfacial adhesion

Figure 4 shows the effects of plasma-treatment power on ILSS of the Armos-fiber-reinforced PPESK composite. The ILSS of the untreated composite was 59.5 MPa. However, after 120-W plasma treatment, ILSS of the composite increased to 64.9 MPa, an increment of about 9%. In addition, ILSS of the composite kept increasing up to the 200-W plasma treatment. These results suggest that plasma treatment significantly enhanced the interfacial adhesion of the Armos-fiber-reinforced PPESK composite by introducing some polar groups to the Aramid fiber surface and by increasing the fiber surface roughness.[20]

CONCLUSIONS

Oxygen plasma treatment was applied to modify the Armos fiber surface for improving the interfacial adhesion between the high-performance fiber and a kind of advanced thermoplastic matrix, PPESK. Different plasma-treatment powers on the fiber surface and the composite interfacial properties were investigated. The SEM and AFM results show that the fiber surface morphology was roughened and that the surface roughness increased after oxygen plasma treatments with powers lower than 200 W. XPS analysis indicated that surface carbon concentration decreased and the oxygen concentration increased after oxygen plasma treatment. The introduced oxygen element reacted with the fiber surface atoms and then formed oxygen-containing functional groups, such as —C=O and —COO—, which improved the fiber surface wettability and enhanced the composite interfacial adhesion. DCAA results proved that surface wettability improved largely after oxygen plasma treatment. The contact angles with water decreased obviously and the surface free energy increased accordingly. The ILSS values of the plasma-treated fiber samples under various plasma-treatment powers were enhanced. However, greater powers, as high as 240 W, did not improve ILSS further. Therefore, we concluded that there existed an optimum plasma treatment condition.

References

1. Coffey, A. B.; Bradaigh, C. M. O.; Young, R. J. J Mater Sci 2007, 42, 8053.
2. Chen, P.; Wang, J.; Wang, B. C.; Li, W.; Zhang, C. S.; Li, H.; Sun, B. L. Surf Interface Anal 2009, 41, 38.
3. Seo, M. K.; Park, S. J. J Colloid Interface Sci 2009, 330, 237.
4. Wu, J.; Cheng, X. H. J Appl Polym Sci 2006, 102, 4165.
5. Wu, S. R.; Sheu, G. S.; Shyu, S. S. J Appl Polym Sci 1996, 62, 1347.
6. De Lange, P. J.; Akker, P. G.; Mader, E. Compos Sci Technol 2007, 67, 2027.
7. Day, R. J.; Hewson, K. D.; Lovell, P. A. Compos Sci Technol 2002, 62, 153.
8. Maity, J.; Jacob, C.; Das, C. K. J Appl Polym Sci 2008, 107, 3739.
9. Liu, L.; Jiang, Q.; Zhu, T. J Appl Polym Sci 2006, 102, 242.
10. Yip, J.; Chan, K.; Sin, K. M. Polym Int 2004, 53, 634.
11. Brown, J. R.; Mathys, Z. J Mater Sci 1997, 32, 2599.
12. Wang, J.; Chen, P.; Li, H.; Li, W.; Wang, B. C.; Zhang, C. S.; Ren, N. Surf Interface Anal 2008, 40, 1299.
13. Yip, J.; Chan, K.; Sin, K. M. Appl Surf Sci 2006, 253, 2493.
14. Park, J. M.; Kim, D. S.; Kim, S. R. J Colloid Interface Sci 2003, 264, 431.
15. Chen, P.; Zhang, C. S.; Wang, J. Chin. Pat. 2006, ZL200610134662.3.
16. Žukienė, K.; Jankauskaitė, V.; Petraitienė S. Appl Surf Sci 2006, 253, 966.
17. Lu, C.; Chen, P.; Yu, Q.; Ding, Z. F.; Lin, Z. W.; Li, W. J Appl Polym Sci 2007, 106, 1733.
18. Zhang, Y. H.; Huang, Y. D.; Liu, L.; Wu, L. N. J Appl Polym Sci 2007, 106, 2251.
19. Chen, P.; Zhang, C. S.; Zhang, X. Y.; Wang, B. C.; Li, W.; Lei, Q. Q. Appl Surf Sci 2008, 255, 3153.
20. Wang, J.; Chen, P.; Li, H.; Zhang, C. S.; Sun, B. L.; Zhang, X. Y. Surf Coat Technol 2008, 202, 4986.